/3mi4

NASA TECHNICAL MEMORANDUM

NASA TM X- 71962

COPY NO.

NASA TM X- 71962

ANALYSIS OF THE FEEDBACK SYSTEM IN A NONINTRUSIVE DYNAMIC FLOWMETER FOR MEASURING POGO OSCILLATIONS

(NASA-TM-X-71962) ANALYSIS OF THE FEEDBACK SYSTEM IN A NONINTRUSIVE DYNAMIC FLOWMETER FOR MEASURING POGO OSCILLATIONS (NASA) 43 p HC $3.25 CSCL 14B

N74-23054

Unclas

G3/14 39385

BY WILLIAM G. CHAPIN

This informal documentation medium is used to provide accelerated or special release of technical information to selected users. The contents may not meet NASA formal editing and publication standards, may be revised, or may be incorporated in another publication.

NATIONAL AERONAUTICS AND SPACE ADMINISTRATION
LANGLEY RESEARCH CENTER, HAMPTON, VIRGINIA 23665

1. Report No.	2. Government Accession No.	3. Recipient's Catalog No.
NASA TM X-71962		
4. Title and Subtitle ANALYSIS OF THE FEEDBACK SYSTEM IN A NONINTRUSIVE DYNAMIC FLOWMETER FOR MEASURING POGO OSCILLATIONS		5. Report Date 6. Performing Organization Code
7. Author(s) William G. Chapin		8. Performing Organization Report No.
9. Performing Organization Name and Address NASA, Langley Research Center Hampton, VA 23665		10. Work Unit No. 502-32-02-06 11. Contract or Grant No.
12. Sponsoring Agency Name and Address National Aeronautics and Space Administration Washington, DC 20546		13. Type of Report and Period Covered Technical Memorandum 14. Sponsoring Agency Code

15. Supplementary Notes

Interim technical information release, subject to possible revision and/or late formal publication

16. Abstract

Equations are developed which describe the closed loop feedback system operation of a proposed ultrasonic, dynamic, nonintrusive flowmeter whose design is based on a constant phase, voltage controlled frequency feedback concept. These equations are based on linear feedback system theory. The time constant of a low pass filter is taken into account. The equations show that the larger the open loop gain, the smaller the error due to fluctuations in the speed of sound and the smaller the effective time constant.

17. Key Words (Suggested by Author(s)) (STAR category underlined)	18. Distribution Statement
Instrumentation, flowmeter, dynamic, nonintrusive, ultrasonic	Unclassified - Unlimited Star Category

19. Security Classif. (of this report)	20. Security Classif. (of this page)	21. No. of Pages	22. Price*
Unclassified	Unclassified	43	$3.25

*Available from { The National Technical Information Service, Springfield, Virginia 22151
STIF/NASA Scientific and Technical Information Facility, P.O. Box 33, College Park, MD 20740 }

ANALYSIS OF THE FEEDBACK SYSTEM IN A NONINTRUSIVE DYNAMIC FLOWMETER FOR MEASURING POGO OSCILLATIONS

By William G. Chapin
Langley Research Center

SUMMARY

Equations are developed which describe the closed loop feedback system operation of a proposed ultrasonic, dynamic, nonintrusive flowmeter whose design is based on a constant phase, voltage controlled, frequency feedback concept. These equations are based on linear feedback system theory. The time constant of a low pass filter is taken into account. The equations show that the larger the open loop gain, the smaller the error due to fluctuations in the speed of sound and the smaller the effective time constant.

INTRODUCTION

Many liquid-propellant rocket vehicles have experienced longitudinal vibrations because of an instability arising from interaction of the vehicle structure with the propulsion system. These vibrations, nicknamed "Pogo" after the jumping stick, have occurred principally in the first longitudinal structural mode during the first stage of a launch vehicle. The vibration begins spontaneously, intensifies, and then dies away - typically in a period of 10 to 40 seconds.

In the interest of predicting whether or not the Space Shuttle Vehicle will "Pogo" it is necessary to measure the dynamic flow component in the LOX fuel lines during ground testing of the space shuttle main engine. This measurement should identify fluctuations in flow velocity to 100 Hz over a range ± 1.5 m/sec to ± 15 m/sec (± 5 ft/sec to ± 50 ft/sec) with a resolution of .003 m/sec (.01 ft/sec).

Since no flowmeter was available which could meet the stringent requirements of this measurement, one had to be developed under an R&D design study contract as reported in NASA CR-112313 (ref. 1). This flowmeter operates on the principle of propagating two continuous ultrasonic sound waves (one upstream and one downstream) through the flowing medium by means of externally mounted transducer-receivers, (fig. 1). This flowmeter apparently meets the requirements of nonintrusiveness, fast response, high accuracy and high resolution, and was designed to measure flow rates in cryogenic liquids and water. The heart of this flowmeter is its closed loop feedback system which represents the state-of-the-art in flow technology.

Reference 1 contains an analysis of the flowmeter design concept, along with a block diagram of the electronics and some circuit and mechanical details; however, reference 1 contains no analysis of the closed loop feedback system operation. It was concluded that an analysis of the closed loop feedback system operation was needed to determine how or to what extent the system would actually produce the behavior described in the reference 1 design analysis. Such an understanding was considered necessary to the effective evaluation of the design concept. For example, in reference 1, it is shown that the propagation of both an upstream wave and a downstream wave would, by means of a cancellation process, eliminate a measurement error due to fluctuations in the speed of sound in the flow medium. The question arose as to whether complete cancellation or only partial cancellation is an inherent feature of the actual system. It was realized that a mathematical model of the closed loop feedback system would be very helpful in answering this question.

In this report, such a model is developed. It is based on classical linear feedback system theory and small fluctuations about a static operating point.

First, the pertinent aspects of the analysis of reference 1 are presented. It shows that the simultaneous transmission of a downstream and an upstream wave results, ideally, in the elimination of fluid velocity measurement errors due to fluctuations in the speed of sound. Then the analysis of the closed loop servo operation is presented with appropriate servo block diagrams depicting the transfer functions and supporting equations.

SYMBOLS

A	amplitude of the voltage controlled oscillator (VCO) output
c	velocity of sound
D	tube diameter
f_1, f_2	frequencies of downstream and upstream systems, respectively
f_{10}, f_{20}	fixed components of the frequencies of the downstream and upstream systems, respectively
F_1, F_2	variable components of the frequencies of the downstream and upstream systems, respectively
K_a	gain constant of dc amplifiers
K_f	gain constant of low pass filters
K_m	gain constant of multipliers
K_ϕ	gain constant of transmitter-receivers
K_1, K_2	gain constants relating the voltage to the variable frequency component of the VCO units for the downstream and upstream systems, respectively
K_3, K_4, K_5, K_6	gain constants of the various flowmeter components as shown in figure 3.
M, N	integers
out (n)	output at a block in figure 3, where n represents the number of the block.
S	Laplace operator
t	time
T	time constant of low pass filters
v	velocity of fluid
V_1, V_2	instantaneous outputs of the amplifiers of the downstream and upstream systems, respectively
V_{f1}, V_{f2}	instantaneous outputs of the low pass filters of the downstream and upstream systems, respectively

V_{m1}, V_{m2}	instantaneous outputs of the multipliers of the downstream and upstream systems, respectively
$\tilde{V}_{m1}$	component of V_{m1} assumed not to be completely attenuated by the low pass filter
$\tilde{V}_{m2}$	component of V_{m2} assumed not to be completely attenuated by the low pass filter
θ	acute angle between the direction of wave propagation and the wall of the tube (see fig. 1)
ϕ_1, ϕ_2	phase lags between the transmitter and receiver for downstream and upstream systems, respectively
λ	wave length of the transmitted ultrasonic wave for the downstream system
subscript s	static operating values about which systems operate dynamically
subscript d	dynamic values about the static operating values
superbar, $\bar{}$, over a variable	Laplace transform of the time domain dynamic component of a variable

GENERAL THEORY AND DESCRIPTION OF PROPOSED SYSTEM

The basic purpose of the proposed nonintrusive dynamic flowmeter (ref. 1) is to measure the dynamic flow velocity of liquids in a tube. In figure 1 each transducer contains a transmitter and a receiver. The transmitter of transducer 1 and the receiver of transducer 2 are called the "downstream system." The transmitter of transducer 2 and the receiver of transducer 1 are called the "upstream system." Each of the transmitters is driven by a digital frequency synthesizer. Pertinent aspects of the analysis of the flowmeter design concept contained in reference 1 are summarized next. The important outcome of the analysis is that with suitable adjustment of some system parameters, the difference in voltage outputs of the two systems can be made a function of axial fluid velocity and independent of the speed of sound. This measurement concept represents the ideal behavior to be attained as closely as possible by the actual system.

Consider a wave of frequency f_1 propagated downstream from the transmitter of transducer 1 to the receiver of transducer 2 at an angle θ with the wall of the tube. The phase of the wave at 2 is

$$\phi_1 = \frac{2\pi D}{\sin\theta} \cdot \frac{1}{\lambda}$$

also,

$$\lambda = \frac{c + v\cos\theta}{f_1}$$

If these equations are combined, there is obtained

$$\phi_1 = \frac{2\pi D f_1}{(c + v\cos\theta)\sin\theta} \qquad (1)$$

In the anticipated applications, it has been estimated that with a single frequency system, a change in pressure of only 10^{-3} atmospheres would cause a variation in the speed of sound such that the resolution specification of .003 m/sec would be exceeded. Pressure variations are very likely to be considerably more than this, not to mention other sources of variation in the speed of sound. To minimize the effect of changing sound speed, a wave is also propagated upstream from the transmitter of transducer 2 to the receiver of transducer 1. Here

$$\phi_2 = \frac{2\pi D f_2}{(c - v \cos \theta) \sin\theta} \tag{2}$$

For the downstream system, an increase in fluid velocity tends to decrease the phase angle, while for the upstream system, such an increase tends to increase the phase angle. On the other hand, for each system, an increase in the speed of sound tends to decrease the phase angle. The frequency f_1 consists of a fixed frequency f_{10} plus a voltage controlled frequency F_1. The latter F_1 is caused to vary so that

$$\phi_1 = \frac{\pi}{2} (2N - 1) \tag{3}$$

This is an idealized relationship, since, as is shown later at least a small deviation of ϕ_1 from $\frac{\pi}{2}$ (2N-1) is an inherent feature of the servo system.

Similarly, f_2 consists of a fixed component, f_{20} plus a variable component F_2 such that, ideally,

$$\phi_2 = \frac{\pi}{2} (2M - 1) \tag{4}$$

The frequency f_{10} is selected to be 1 MHz and f_{20} is set at 1.1 MHz.

Equations (1) and (2) can be rewritten as

$$\phi_1 = \frac{2\pi D(f_{10} + F_1)}{(c + v \cos \theta) \sin \theta} \tag{5}$$

$$\phi_2 = \frac{2\pi D(f_{20} + F_2)}{(c - v \cos \theta) \sin \theta} \tag{6}$$

If the right sides of (3) and (5) are equated and the resulting equation is solved for F_1, there is obtained

$$F_1 = \frac{(2N-1) \sin \theta}{4D} (c + v \cos \theta) - f_{10} \tag{7}$$

Similarly, from (4) and (6), there is obtained

$$F_2 = \frac{(2M-1) \sin \theta}{4D} (c - v \cos \theta) - f_{20} \tag{8}$$

By operating the digital frequency synthesizers in the frequency modulation mode, F_1 and F_2 can be made proportional to voltage inputs to the synthesizer .

That is

$$F_1 = K_1 V_1 \tag{9}$$

and

$$F_2 = K_2 V_2 \tag{10}$$

Furthermore, to obtain an output independent of the speed of sound, it is necessary to adjust K_1 and K_2 so that

$$K_2 = K_1 \left(\frac{2M-1}{2N-1} \right) \tag{11}$$

Finally, from equations (7) through (11), an equation is evolved which relates a voltage output, $V_1 - V_2$, to the axial fluid velocity v:

$$V_1 - V_2 = \frac{(2N-1)}{K_1} \left(\frac{\sin \theta \cos \theta}{2D} \right) v - \left[\frac{f_{10}}{K_1} - \frac{f_{20}}{K_1} \left(\frac{2N-1}{2M-1} \right) \right] \tag{12}$$

Here the troublesome speed-of-sound variable cancels out and the last term is merely a dc bias. Equation (12) then represents the ideal behavior to be attained by the actual flowmeter system.

DEVELOPMENT OF THE LINEAR FEEDBACK MODEL

Figure 2 is a simplified diagram of one channel of the proposed flowmeter (appendix G, ref. 1). Notation is that pertaining to the downstream system which is analyzed in some detail. Figure 3 shows the more detailed block diagram of the flowmeter (ref. 1, page 57). The "Filter" of figure 2 corresponds to the "LPF" (Low Pass Filter) of figure 3. An analysis is first made of the simplified system of figure 2, after which it is shown that the system of figure 3 essentially corresponds to that of figure 2. The relationships for the upstream system are easily obtained from the results of the analysis of the downstream system.

On various occasions, use is made of the following trigonometric identities:

$$\sin a \sin b = \frac{1}{2} \cos (a - b) - \frac{1}{2} \cos (a + b) \tag{I.1}$$

$$\cos a \cos b = \frac{1}{2} \cos (a - b) + \frac{1}{2} \cos (a + b) \tag{I.2}$$

The 1/2 term does not explicitly appear in any equations since it can be included as part of a gain constant.

Analysis of Downstream System

For the downstream system (fig. 2), equations which express pertinent instantaneous time relationships are now restated or developed.

The inputs to the multiplier are the reference wave and the reference wave delayed in phase by ϕ_1, and as (I.1) implies,

$$V_{m1} = K_m' \left[A \sin 2\pi(F_1 + f_{10}) t\right] \left[K_\phi A \sin \left(2\pi(F_1 + f_{10}) t - \phi_1\right)\right]$$

$$= K_m K_\phi A^2 \cos \phi_1 - K_m K_\phi A^2 \cos \left[2\pi(2F_1 + 2f_{10}) t - \phi_1\right]$$

where $K_m = K_m'/2$

If it is assumed that, in passing through the filter, the high frequency component is completely eliminated, the component of interest would become

$$\tilde{V}_{m_1} = K_m K_\phi A^2 \cos \phi_1 \tag{13}$$

As shown previously,

$$\phi_1 = \frac{2\pi D(F_1 + f_{10})}{\sin \theta (c + v \cos \theta)} \tag{5}$$

It is planned to make the time constant, T, of the low pass filter about .01 seconds (ref. 1), which implies that the response is down 3 db at about 16 Hz. Therefore, the output of the filter is a function of the time variation of the input. That is,

$$V_{f_1} (t) = V_{f_1} [\tilde{V}_{m_1} (t)] \tag{14}$$

Since the maximum frequency of interest is 100 Hz, it is assumed that any time constants of the amplifier are insignificant. Hence,

$$V_1 = K_a V_{f_1} \tag{15}$$

and, as stated previously,

$$F_1 = K_1 V_1 \tag{9}$$

If small fluctuations in c and v about a static operating point are assumed, the dynamic relationships can be considered to be equivalent to the differential relationships. Then from equation (5)

$$d\phi_1 = \left[\frac{\partial \phi_1}{\partial F_1} \cdot dF_1 + \frac{\partial \phi_1}{\partial c} \cdot dc + \frac{\partial \phi_1}{\partial v} \cdot dv \right]$$

and with

$$F_1 = F_{1s}, \quad v = v_s \quad \text{and} \quad c = c_s$$

then

$$d\phi_1 = \frac{2\pi D}{\sin\theta\,(c_s + v_s\cos\theta)}\,dF_1 + \frac{2\pi D}{\sin\theta}\,(F_{1s} + f_{10})(c_s + v_s\cos\theta)^{-2}(-1)dc$$

$$+ \frac{2\pi D}{\sin\theta}\,(F_{1s} + f_{10})(c_s + v_s\cos\theta)^{-2}(-1)(\cos\theta)dv$$

or

$$d\phi_1 = \frac{2\pi D}{\sin\theta(c_s + v_s\cos\theta)}\,dF_1 - \frac{2\pi D(F_{1s} + f_{10})}{\sin\theta\,(c_s + v_s\cos\theta)^2}\,dc$$

$$- \frac{2\pi D(F_{1s} + f_{10})\cos\theta}{\sin\theta\,(c_s + v_s\cos\theta)^2}\,dv$$

If the subscript "d" is used to denote the dynamic component, the preceding equation can be rewritten as,

$$\phi_{1d}(t) = \frac{2\pi D}{\sin\theta\,(c_s + v_s\cos\theta)}\,F_{1d}(t) - \frac{2\pi D(F_{1s} + f_{10})}{\sin\theta\,(c_s + v_s\cos\theta)^2}\,c_d(t)$$

$$- \frac{2\pi D(F_{1s} + f_{10})\cos\theta}{\sin\theta\,(c_s + v_s\cos\theta)^2}\,v_d(t) \tag{16}$$

Likewise from equation (13)

$$d\tilde{V}_{m_1} = -K_m K_\phi\,A^2\,(\sin\phi_1)d\phi_1$$

which implies $V_{mld}(t) = -K_m K_\phi\ A^2(\sin \phi_{1s})\ \phi_{1d}(t)$ (17)

Also from equations (14), (15), and (9)

$$V_{fld}(t) = V_{fld}[\tilde{V}_{mld}\ (t)] \tag{18}$$

$$V_{1d}(t) = K_a V_{fld}(t) \tag{19}$$

$$F_{1d}(t) = K_1\ V_{1d}(t) \tag{20}$$

Now take the Laplace transforms of equations (16) through (20)

$$\bar{\phi}_{1d}(S) = \frac{2\pi D}{\sin \theta(c_s + v_s \cos \theta)} \bar{F}_{1d}(S) - \frac{2\pi D(F_{1s} + f_{10})}{\sin \theta(c_s + v_s \cos \theta)^2} \bar{c}_d(S)$$

$$- \frac{2\pi D(F_{1s} + f_{10}) \cos \theta}{\sin \theta(c_s + v_s \cos \theta)^2} \bar{v}_d(S) \tag{21a}$$

or

$$-\bar{\Phi}_{1d}(S) = \frac{-2\pi D}{\sin \theta(c_s + v_s \cos \theta)} \bar{F}_{1d}(S) + \frac{2\pi D(F_{1s} + f_{10})}{\sin \theta(c_s + v_s \cos \theta)^2} \bar{c}_d(S)$$

$$+ \frac{2\pi D(F_{1s} + f_{10}) \cos \theta}{\sin \theta(c_s + v_s \cos \theta)^2} \bar{v}_d(S) \tag{21b}$$

For the multiplier, the S domain equation for the dynamic voltage output is

$$\bar{\tilde{V}}_{mld}(S) = K_m K_\phi\ A^2(\sin \phi_{1s})\ (-\bar{\Phi}_{1d}(S)) \tag{22}$$

For the filter,

$$\bar{V}_{fld}(S) = \frac{K_f}{TS + 1} \cdot \bar{\bar{V}}_{mld}(S) \tag{23}$$

and for the output amplifier,

$$\bar{V}_{ld}(S) = K_a \bar{V}_{fld} (S) \tag{24}$$

The S domain equation for the controlling frequency is

$$\bar{F}_{ld}(S) = K_1 \bar{V}_{ld} (S) \tag{25}$$

Equations (21b) through (25) can be represented by the block diagram shown in figure 4. It is desired to transform the configuration shown in figure 4 to a configuration of the form shown in figure 9. To do this, the general block diagram transformations shown in figure 5 are used.

The diagram shown in figure 6 is derived from that shown in figure 4 by applying transformation T.1 to the blocks in the forward loop and T.3 to the blocks immediately ahead of the inputs. The diagram shown in figure 7 is derived from that shown in figure 6 by applying transformation T.2 to the block to the left of the feedback loop. Finally, the block diagram shown in figure 8 is derived from that of figure 7 by use of transformation T.1. The diagram shown in figure 8 has the desired configuration. R in figure 9 corresponds to $\bar{c}_d (S) + (\cos \theta)\bar{v}_d(S)$ in figure 8.

For a negative feedback system represented by the block diagram shown in figure 9, the relationship between the output C and the input R is

$$C = \frac{G}{1 + GH} R, \text{ which implies that}$$

$$\bar{V}_{1d}(S) = \frac{\dfrac{K_a K_f K_m K_\phi\ A^2(\sin\phi_{1s})2\pi D(F_{1s} + f_{10})}{\sin\theta(c_s + v_s\cos\theta)^2(TS + 1)}}{1 + \dfrac{K_1 K_a K_f K_m K_\phi\ A^2(\sin\phi_{1s})2\pi D}{\sin\theta(c_s + v_s\cos\theta)(TS + 1)}}\ (\bar{c}_d(S) + (\cos\theta)\bar{v}_d(S)) \tag{26a}$$

or

$$\bar{V}_{1d}(S) = \frac{\dfrac{K_a K_f K_m K_\phi\ A^2(\sin\phi_{1s})(2\pi D)(F_{1s} + f_{10})}{\sin\theta(c_s + v_s\cos\theta)^2}}{TS+1 + \dfrac{K_1 K_a K_f K_m K_\phi\ A^2(\sin\phi_{1s})2\pi D}{\sin\theta(c_s + v_s\cos\theta)}}\ (\bar{c}_d(S) + (\cos\theta)\bar{v}_d(S)) \tag{26b}$$

The question arises as to what is the sign of $\sin\phi_{1s}$. At present, it is assumed that the magnitude of the right hand term of the denominator of equation (26a) is to be made >>1. It is shown later that this is a necessary condition for the desired operation of the flowmeter. Inspection of equation (26b) reveals that if $\sin\phi_{1s}$ is negative, there would be a pole in the right hand plane which would result in an unstable system. An analysis of this problem is presented next.

It is assumed that no dynamic fluctuations are present but that, for some reason, ϕ_1 is not at the static operating point ϕ_{1s}. If ϕ_1 were in either the second or the third quadrant, then $\cos\phi_1$ would be negative. Inspection of equations (13), (5), (14), (15) and (9) reveals that the output of the multiplier $\tilde{V}_{m1}$ would be negative, as would be V_{f1} and, therefore, V_1. A negative V_1 would cause F_1 to decrease which, in turn, would cause ϕ_1 to decrease. Consequently, the system would drive toward the design static operating condition $\phi_1 = (2N - 1)\frac{\pi}{2}$, where N is odd. Therefore, $\sin\phi_{1s}$ would be positive. If, on the other hand, ϕ_1 were in either the fourth or the first quadrant, then $\cos\phi_1$ would be positive which would cause F_1 to increase. Consequently, ϕ_1 would increase, and the system would again drive toward the condition $\phi_1 = (2N - 1)\frac{\pi}{2}$, where N is odd. Therefore, sin ϕ_{1s} would again be positive. If, for some reason, ϕ_1 were to exactly equal $(2N - 1)\frac{\pi}{2}$, where N is even, it seems likely that very soon some external or internal disturbance would occur and the nulling process would be triggered.

In the remainder of this report, it is assumed that N and M (for the upstream system) are odd.

The static operating point, ϕ_{1s}, would not be exactly at $(2N - 1)\frac{\pi}{2}$ because a non zero cos ϕ_1 is needed to produce at least a small multiplier output voltage, $\tilde{V}_{m1}$, so that the amplifier can maintain the required non zero variable frequency component F_1. An equation is now developed which relates this difference between ϕ_{1s} and $(2N - 1)\frac{\pi}{2}$ to system parameters. First one must rewrite equations (13), (5), (14), (15), and (9) in terms of values at the static operating point:

$$\tilde{V}_{m1s} = K_m K_\phi A^2 \cos \phi_{1s} \tag{27}$$

$$\phi_{1s} = \frac{2\pi D(F_{1s} + f_{10})}{\sin \theta(c_s + v_s \cos \theta)} \tag{28}$$

$V_{f1s} = V_{f1s}(\tilde{V}_{m1s}) = K_f \tilde{V}_{m1s}$, since static flow conditions are assumed. (29)

Furthermore

$$V_{1s} = K_a V_{f1s} \tag{30}$$

and

$$F_{1s} = K_1 V_{1s} \tag{31}$$

The difference between $(2N - 1)\frac{\pi}{2}$ and ϕ_{1s} can be written

$$\Delta\phi_1 = \frac{\pi}{2}(2N - 1) - \phi_{1s} \tag{32a}$$

which implies

$$\phi_{1s} = \frac{\pi}{2} \; (2N - 1) - \Delta\phi_1 \tag{32b}$$

Then from equations (32a) and (28)

$$\Delta\phi_1 = \frac{\pi}{2} (2N - 1) - \frac{2\pi D \; F_{1s}}{\sin \theta(c_s + v_s \cos \theta)} - \frac{2\pi D \; f_{10}}{\sin \theta(c_s + v_s \cos \theta)} \tag{33}$$

From equation (32b), $\cos \phi_{1s} = \cos (\frac{\pi}{2} (2N - 1) - \Delta\phi_1)$ or $\cos \phi_{1s} = \sin \Delta\phi_1$. If $\sin \Delta\phi_1$ is expanded in a MacLauren series, there is obtained

$$\cos \phi_{1s} = \sin \Delta\phi_1 = \Delta\phi_1 - \frac{(\Delta\phi_1)^3}{3!} + \ldots$$

Therefore, equation (27) becomes

$$\tilde{V}_{m1s} = K_m K_\phi \; A^2(\Delta\phi_1 - \frac{(\Delta\phi_1)^3}{3!} + \ldots) \tag{34}$$

From equations (34), (29), (30), and (31)

$$F_{1s} = K_1 K_a K_f K_m K_\phi \; A^2(\Delta\phi_1 - \frac{(\Delta\phi_1)^3}{3!} + \ldots) \tag{35}$$

The phase angle, ϕ_{10}, attained by the system at $F_1 = 0$ is

$$\phi_{10} = \frac{2\pi D \; f_{10}}{\sin \theta(c_s + v_s \cos \theta)} \tag{36}$$

If equations (35) and (36) are substituted into (33), it becomes

$$\Delta\phi_1 = \frac{\pi}{2}(2N - 1) - \frac{2\pi D\, K_1 K_a K_f K_m K_\phi\, A^2}{\sin\theta(c_s + v_s\cos\theta)}\,\Delta\phi_1$$

$$+ \frac{2\pi D\, K_1 K_a K_f K_m K_\phi\, A^2}{\sin\theta(c_s + v_s\cos\theta)}\left[\frac{(\Delta\phi_1)^3}{3!} - \ldots\right] - \phi_{10}$$

or

$$\Delta\phi_1\left[1 + \frac{2\pi D\, K_1 K_a K_f K_m K_\phi\, A^2}{\sin\theta(c_s + v_s\cos\theta)}\right] = \frac{\pi}{2}(2N - 1) - \phi_{10}$$

$$+ \frac{2\pi D\, K_1 K_a K_f K_m K_\phi\, A^2}{\sin\theta(c_s + v_s\cos\theta)}\left[\frac{(\Delta\phi_1)^3}{3!} - \ldots\right]$$

or

$$\Delta\phi_1 = \frac{\frac{\pi}{2}(2N - 1) - \phi_{10}}{1 + \frac{2\pi D\, K_1 K_a K_f K_m K_\phi\, A^2}{\sin\theta(c_s + v_s\cos\theta)}} + \frac{\frac{2\pi D\, K_1 K_a K_f K_m K_\phi\, A^2}{\sin\theta(c_s + v_s\cos\theta)}\left[\frac{(\Delta\phi_1)^3}{3!} - \ldots\right]}{1 + \frac{2\pi D\, K_1 K_a K_f K_m K_\phi\, A^2}{\sin\theta(c_s + v_s\cos\theta)}}$$

or

$$\Delta\phi_1 - \frac{\frac{2\pi D\, K_1 K_a K_f K_m K_\phi\, A^2}{\sin\theta(c_s + v_s\cos\theta)}\left[\frac{(\Delta\phi_1)^3}{3!} - \ldots\right]}{1 + \frac{2\pi D\, K_1 K_a K_f K_m K_\phi\, A^2}{\sin\theta(c_s + v_s\cos\theta)}} = \frac{\frac{\pi}{2}(2N - 1) - \phi_{10}}{1 + \frac{2\pi D\, K_1 K_a K_f K_m K_\phi\, A^2}{\sin\theta(c_s + v_s\cos\theta)}} \tag{37a}$$

Comparison of the denominator on the right side of equation (37a) with that of (26a) reveals that it is 1+ the open loop gain constant, except for the sin ϕ_{1s} term of the latter equation. Assume, more specifically, that the system is designed such that

$$\frac{2\pi\ D\ K_1\ K_a\ K_f\ K_m\ K_\phi\ A^2}{\sin\ \theta\ (c_s + v_s\ \cos\ \theta)} >> 1$$

which implies that the second term on the left hand side of equation (37a)

$$\doteq -\left(\frac{(\Delta\phi_1)^3}{3!} - \ldots\right).$$ At most, $\frac{\pi}{2}(2N-1) - \phi_{10} = \pm\ \pi$ radians.

Therefore $$\left|\Delta\phi_1 - \frac{(\Delta\phi_1)^3}{3!} + \ldots\right|_{max} \doteq \frac{\pi}{1 + \frac{2\pi D\ K_1 K_a K_f K_m K_\phi\ A^2}{\sin\ \theta(c_s + v_s\ \cos\ \theta)}} \qquad (37b)$$

Further, the right hand side of equation (37b) is $<< 1$, yielding the relationship

$$\left|\frac{(\Delta\phi_1)^3}{3!} - \ldots\right| << \left|\Delta\phi_1\right|$$

and equation (37b) can be written

$$\left|(\Delta\phi_1)\right|_{max} \doteq \frac{\pi}{1 + \frac{2\pi D\ K_1 K_a K_f K_m K_\phi\ A^2}{\sin\ \theta(c_s + v_s\ \cos\ \theta)}} << 1 \qquad (37c)$$

which implies that

$$\phi_{1s} \doteq \frac{\pi}{2}(2N-1) \tag{38a}$$

$$\sin \phi_{1s} \doteq 1 \tag{38b}$$

Equation (38a) verifies that, for static conditions, the idealized condition stated by equation (3) will be closely attained.

Simplified expressions for equations (26a) and (26b) can be obtained; From equations (28) and (38a)

$$\phi_{1s} = \frac{2\pi D(F_{1s} + f_{10})}{\sin \theta(c_s + v_s \cos \theta)} \doteq \frac{\pi}{2}\ (2N - 1)$$

which implies

$$(F_{1s} + f_{10}) \doteq \frac{\pi}{2}(2N - 1) \left[\frac{\sin \theta(c_s + v_s \cos \theta)}{2\pi D}\right]$$

$$= \frac{(2N - 1) \sin \theta(c_s + v_s \cos \theta)}{4D} \tag{39}$$

The block diagram obtained by applying equations (38b) and (39) to figure 8 is shown in figure 10.

Equations (26a) and (26b), which relate system output to inputs,now become

$$\bar{V}_{1d}(S) = \frac{\dfrac{K_a K_f K_m K_\phi A^2(2N - 1)\pi}{2(c_s + v_s \cos \theta)(TS + 1)}}{1 + \dfrac{2\pi D\ K_1 K_a K_f K_m K_\phi A^2}{\sin \theta(c_s + v_s \cos \theta)(TS + 1)}} \left(\bar{c}_d(S) + (\cos \theta)\bar{v}_d(S)\right) \tag{40a}$$

or

$$\bar{V}_{1d}(S) = \frac{\dfrac{K_a K_f K_m K_\phi A^2 \ (2N - 1) \ \pi}{2(c_s + v_s \cos \theta)}}{TS + 1 + \dfrac{2\pi D \ K_1 K_a K_f K_m K_\phi \ A^2}{\sin \ \theta(c_s + v_s \cos \ \theta)}} \left(\bar{c}_d(S) + (\cos \ \theta)\bar{v}_d(S)\right) \tag{40b}$$

The denominator is of the form

$$TS + 1 + K = (1 + K) \left[\frac{TS}{1 + K} + 1\right]$$

This shows that the effective time constant of the closed loop system is reduced by the factor $1 + K$, where K is the open loop gain constant.

Analysis of Upstream System

For the upstream system, the analysis makes use of the instantaneous equations:

$$\tilde{V}_{m2} = K_m K_\phi \ A^2 \cos \ \phi_2 \tag{41}$$

$$\phi_2 = \frac{2\pi D(F_2 + f_{20})}{\sin \ \theta(c - v \cos \ \theta)} \tag{6}$$

$$V_{f2}(t) = V_{f2} \ \ (\tilde{V}_{m2}(t)) \tag{42}$$

$$V_2 = K_a \ V_{f2} \tag{43}$$

$$F_2 = K_2 \ V_2 \tag{10}$$

The analysis of this upstream system is similar to that of the downstream system; however, whereas in the downstream system, an increase in fluid velocity tends to cause a decrease in phase angle, in this upstream system, an increase in fluid velocity tends to cause an increase in phase angle. Thus,

$$\phi_{2d}(t) = \frac{2\pi D\ F_{2d}(t)}{\sin\ \theta(c_s - v_s\ \cos\ \theta)} - \frac{2\pi D(F_{2s} + f_{20})}{\sin\ \theta(c_s - v_s\ \cos\ \theta)^2} \cdot c_d(t)$$

$$+ \frac{2\pi D\ (F_{2s} + f_{20})(\cos\ \theta)}{\sin\ \theta(c_s - v_s\ \cos\ \theta)^2} \cdot v_d(t) \tag{44}$$

In the S domain

$$-\bar{\phi}_{2d}(S) = -\frac{2\pi D\ \bar{F}_{2d}\ (S)}{\sin\ \theta(c_s - v_s\ \cos\ \theta)} + \frac{2\pi D\ (F_{2s} + f_{20})}{\sin\ \theta(c_s - v_s\ \cos\ \theta)^2} \cdot \bar{c}_d(S)$$

$$- \frac{2\pi D(F_{2s} + f_{20})(\cos\ \theta)}{\sin\ \theta(c_s - v_s\ \cos\ \theta)^2} \cdot \bar{v}_d(S) \tag{45}$$

The other Laplace-transformed dynamic equations are:

$$\bar{\tilde{V}}_{m2d}(S) = K_m K_\phi A^2\ \sin\ \phi_{2s}\ (-\bar{\phi}_{2d}(S)) \tag{46}$$

$$\bar{V}_{f2d}(S) = \frac{K_f}{TS + 1} \cdot \bar{\tilde{V}}_{m2d}(S) \tag{47}$$

$$\bar{V}_{2d}(S) = K_a \bar{V}_{f2d}\ (S) \tag{48}$$

$$\bar{F}_{2d}(S) = K_2\ \bar{V}_{2d}(S) \tag{49}$$

Equations (45) through (49) can be put into the block form shown in figure 11.

Figure 11, by transformations similar to those used in the downstream system, assumes the form shown in figure 12.

Also, by analogy with equations (38b) and (39), the following relationships are used:

$$\sin \phi_{2s} \doteq 1$$

$$F_{2s} + f_{20} \doteq \frac{\sin \theta}{4D} (2M - 1)(c_s - v_s \cos \theta)$$

Then, from the general output/input relationship for a negative feedback system,

$$\bar{v}_{2d}(S) = \frac{\dfrac{K_a K_f K_m K_\phi A^2(2M - 1)\pi}{2(c_s - v_s \cos \theta)(TS + 1)} \left(\bar{c}_d(S) - (\cos \theta)\, \bar{v}_d(S)\right)}{1 + \dfrac{2\pi D\, K_2 K_a K_f K_m K_\phi A^2}{\sin \theta (c_s - v_s \cos \theta)(TS + 1)}} \tag{50}$$

Analysis of Combined Downstream and Upstream Systems

The block diagrams for the two individual systems of figures 10 and 12 can be combined as shown in figure 13. In the feedback block of the upstream system, K_2 has been expressed in terms of K_1 by use of equation (11).

From equations (40a) and (50)

$$\bar{v}_{1d}(S) - \bar{v}_{2d}(S) = \frac{\dfrac{K_a K_f K_m K_\phi A^2(2N - 1)\pi}{2(c_s + v_s \cos \theta)(TS + 1)} \left(\bar{c}_d(S) + (\cos \theta)\bar{v}_d(S)\right)}{1 + \dfrac{2\pi D\, K_1 K_a K_f K_m K_\phi A^2}{\sin \theta (c_s + v_s \cos \theta)(TS + 1)}}$$

$$- \frac{\dfrac{K_a K_f K_m K_\phi A^2(2M - 1)\pi}{2(c_s - v_s \cos \theta)(TS + 1)} \left(\bar{c}_d(S) - (\cos \theta)\bar{v}_d(S)\right)}{1 + \dfrac{2\pi D\, K_2 K_a K_f K_m K_\phi A^2}{\sin \theta (c_s - v_s \cos \theta)(TS + 1)}} \tag{51}$$

Next, it is shown that, if the open loop gain (GH in figure 9) is $>> 1$, and, if K_1 and K_2 are adjusted for the relationship expressed by equation (11), the ideal output/input relationship expressed by equation (12) is closely attained. If equation (12) which expresses an instantaneous relationship is rewritten to express a dynamic relationship, there is obtained,

$$V_{1d}(t) - V_{2d}(t) = \left(\frac{2N - 1}{K_1}\right) \frac{\sin\theta\cos\theta}{2D} v_d(t) \qquad (52)$$

Equation (52), then, expresses the relationship between dynamic voltage output and dynamic fluid velocity that would be obtained by an ideal system. Equation (12) and therefore, equation (52) assume that K_1 and K_2 are related in the manner expressed by equation (11).

If the right hand terms in each of the denominator expressions are $>> 1$,

$$\bar{V}_{1d}(S) - \bar{V}_{2d}(S) \doteq \frac{(2N - 1)\sin\theta}{4DK_1}\left(\bar{c}_d(S) + (\cos\theta)\,\bar{v}_d(S)\right)$$

$$- \frac{(2M - 1)\sin\theta}{4DK_2}\left(\bar{c}_d(S) - (\cos\theta)\,\bar{v}_d(S)\right)$$

If equation (11) is used for K_2

$$\bar{V}_{1d}(S) - \bar{V}_{2d}(S) \doteq \frac{(2N - 1)\sin\theta}{4DK_1}\left(\bar{c}_d(S) + (\cos\theta)\bar{v}_d(S)\right)$$

$$- \frac{(2M - 1)\sin\theta}{4DK_1\left(\frac{2M - 1}{2N - 1}\right)}\left(\bar{c}_d(S) - (\cos\theta)\bar{v}_d(S)\right)$$

or

$$\bar{V}_{1d}(S) - \bar{V}_{2d}(S) \doteq \frac{(2N - 1)\sin\theta\cos\theta}{2DK_1}\bar{v}_d(S) \qquad (53)$$

In the time domain,

$$V_{1d}(t) - V_{2d}(t) \doteq \frac{(2N - 1)\sin\theta\cos\theta}{2DK_1} v_d(t) \qquad (54)$$

As seen by inspection of figure 13 and equation (54), the system output is inversely proportional to the feedback path gain, $4DK_1/(2N - 1)\sin\theta$. This, of course, is an inherent disadvantage in the use of negative feedback. To obtain large open loop gain, and at the same time, adequate output/input sensitivity, adequate forward path gain is needed. Changes in the static levels of fluid velocity and sound speed, v_s and c_s, change the forward path gain, but high open loop gain reduces this effect.

ANALYSIS OF THE BLOCK DIAGRAM OF THE PROPOSED FLOWMETER

Next, it is shown that the proposed system of figure 3 corresponds essentially to the simplified system (fig. 2) upon which our analysis has been based.

For the sake of simplicity, interactions between the upstream receiver and downstream transmitter and between the downstream receiver and upstream transmitter are neglected.

In figure 3, the signal outputs are shown at various key points in the system. Some of these output equations are developed below where it is felt they might not be easily determined by inspection.

The outputs are denoted by out n where "n" represents the number of the component block shown in figure 3.

$$\text{Out}\ 11 = K_5'(K_3\ A \sin 2\pi f_1 t)\ (K_4K_3^2\ A \sin [2\pi f_2 t - \phi_2 - \alpha])$$

By use of trigometric identity (I.1) and the relationship, $K_5 = K_5'/2$

$$\text{Out}\ 11 = K_5K_4K_3^3\ A^2\ [\cos\ (2\pi f_2 t - \phi_2 - \alpha - 2\pi f_1 t)$$

$$-\ \cos\ (2\pi f_2 t - \phi_2 - \alpha + 2\pi f_1 t)]$$

or

$$\text{Out}\,(11) = K_5K_4K_3^3\ A^2\ \left\{\cos(2\pi[f_2 - f_1]t - \phi_2 - \alpha) - \cos(2\pi[f_1 + f_2]t - \phi_2 - \alpha)\right\}$$

Similarly

$$\text{Out}\,(14) = K_5K_4K_3^3\ A^2\ [\cos(2\pi f_2t - \alpha - 2\pi f_1t + \phi_1) - \cos(2\pi f_2t - \alpha + 2\pi f_1t - \phi_1)]$$

or

$$\text{Out}\,(14) = K_5K_4K_3^3\ A^2 \left\{\cos(2\pi[f_2 - f_1]t - \alpha + \phi_1) - \cos(2\pi[f_2 + f_1]t - \alpha - \phi_1)\right\}$$

and Out (20) is K_6 x the $(f_2 - f_1)$ term of Out (14)

Similarly

$$\text{Out}\,(19) = K_6K_5K_3^4\ A^2\ \cos(2\pi[f_2 - f_1]t - \alpha)$$

$$\text{Out}\,(21) = K_5'\left\{K_6K_5K_4K_3^3\ A^2\cos(2\pi[f_2 - f_1]t - \phi_2 - \alpha)\right\}\left\{K_6K_5K_3^4\ A^2\cos(2\pi[f_2 - f_1]t - \alpha)\right\}$$

By use of trigometric identity (I.2) and the relationship, $K_5 = K_5'/2$,

$$\text{Out}\,(21) = K_6^2K_5^3K_4K_3^7\ A^4\ \left\{\cos(2\pi[f_2 - f_1]t - \phi_2 - \alpha + 2\pi[f_2 - f_1]t - \alpha) + \cos(2\pi[f_2 - f_1]t - \alpha - 2\pi[f_2 - f_1]t + \alpha + \phi_2)\right\}$$

or

$$\text{Out}\,(21) = K_6^2K_5^3K_4K_3^7\ A^4\ \left\{\cos(2\pi\ .\ 2[f_2 - f_1]t - \phi_2 - 2\alpha) + \cos\ \phi_2\right\}$$

Similarly

$$\text{Out}\,(22) = K_6^2K_5^3K_4K_3^7\ A^4\left\{\cos(2\pi \cdot 2[f_2 - f_1]t - 2\alpha + \phi_1) + \cos\ \phi_1\right\}$$

It can be seen from the foregoing equations that, except for constant terms:

1. Equation (9) holds for both the actual system and the simplified system.
2. The unfiltered part of the output of (22) corresponds to equation (13).
3. The output of (23) corresponds to equation (14).
4. The output of (24) corresponds to equation (15).
5. Equation (5), of course, holds for both the actual and simplified systems.

Similarly, for the upstream system, equation (10) holds for both the actual system and the simplified system and :

1. The unfiltered part of the output of (21) corresponds to equation (41).
2. The output of (25) corresponds to equation (42).
3. The output of (26) corresponds to equation (43).
4. Equation (6), of course, holds for both the actual and the simplified systems.

CONCLUDING REMARKS

An analysis of the feedback system used in servoing the transmitting frequencies of the Panametrics, Inc. dynamic ultrasonic flowmeter has been made. The analysis is based on the assumption that small fluctuations in the speed of sound and axial fluid velocity occur about a static operating point representing a steady-state fluid flow rate.

The analysis reveals that the design concept is essentially sound as long as the open loop gain can be made >>1. This condition is needed to cancel out errors due to fluctuations in the speed of sound and to decrease the flowmeter's effective time constant needed to obtain that frequency response to at least 100 Hz. For example, an open loop gain of 100 results in an effective time constant of 10^{-4} seconds. Further, adequate forward gain is needed to obtain the desired output/input sensitivity, and at the same time, obtain the high open loop gain required for stability. Unfortunately, the forward gain varies with variations in the static (steady-state flow rate) operating values of fluid velocity and sound speed, v_s and c_s, respectively, but high open loop gain reduces this effect also.

Based on the root locus stability criteria, the flowmeter's servoing was found to contain only a single pole in the left hand plane and is inherently stable.

As a result of this analysis, the flowmeter's innovative concept, it is felt, will be more clearly understood and its ability to measure oscillatory flows more effectively evaluated.

REFERENCES

1. Pedersen, Norman E., Lynnworth, Lawrence C., and Carnevale, Edmund H.: Nonintrusive Dynamic Flowmeter. Final Report, June 1973, NAS1-11756, NASA CR - 112313
2. Ogata, Katsuhiko: Modern Control Engineering. Prentice-Hall, Inc., 1970, pp 92-93.

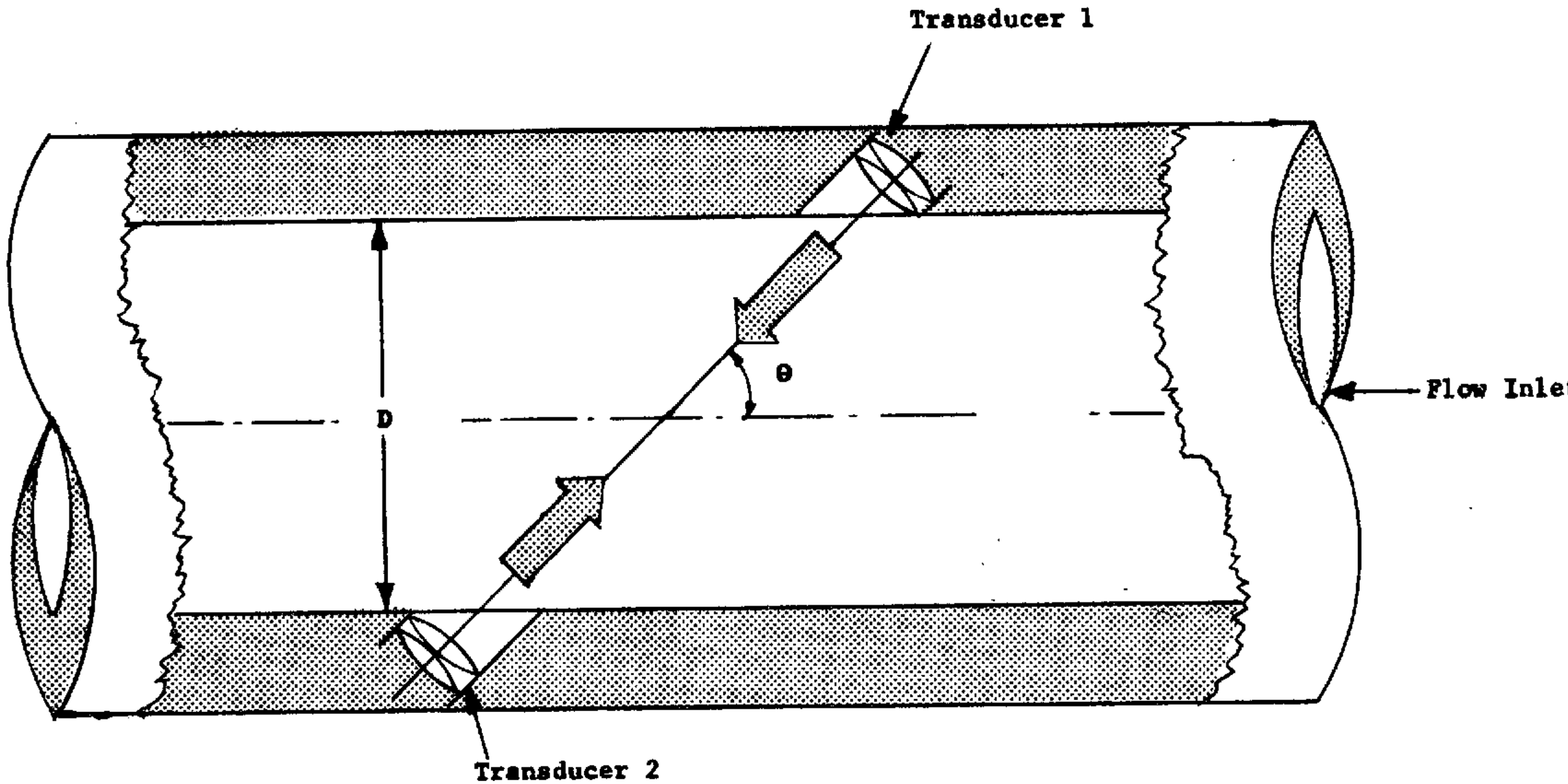

Figure 1. Basic flowmetering geometry.

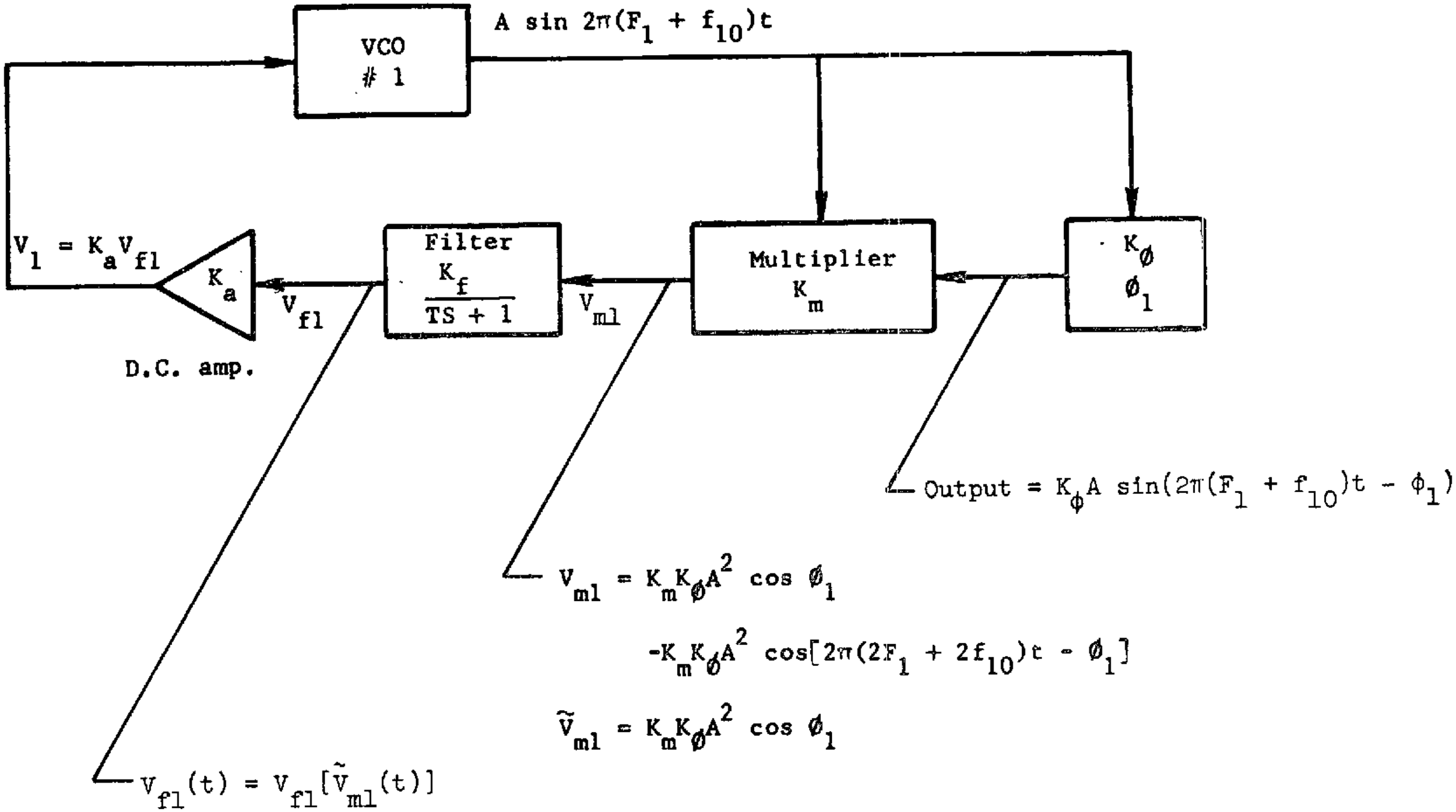

Figure 2. Simplified operational diagram of flowmeter.

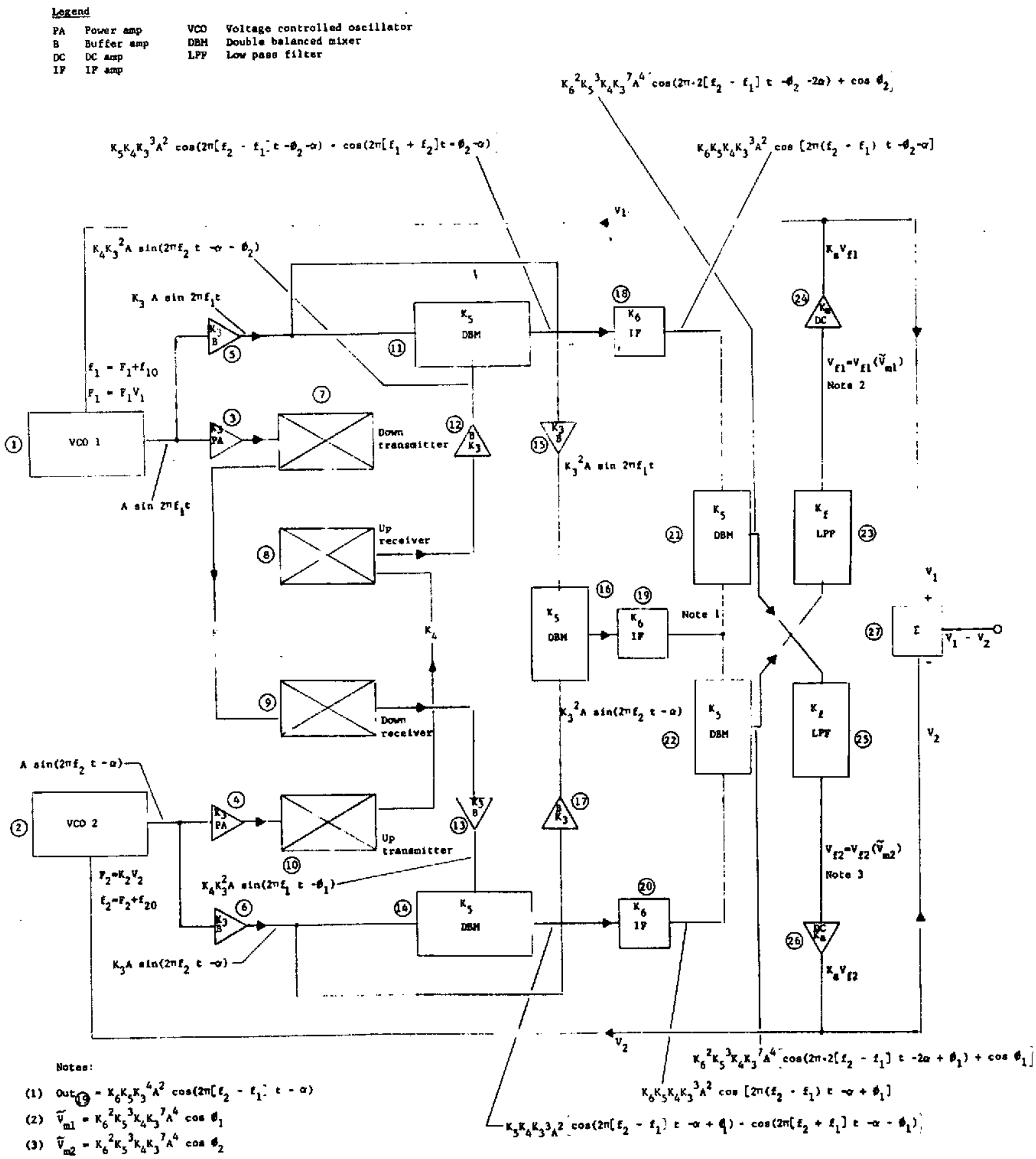

Figure 3. Block diagram of flowmeter electronics.

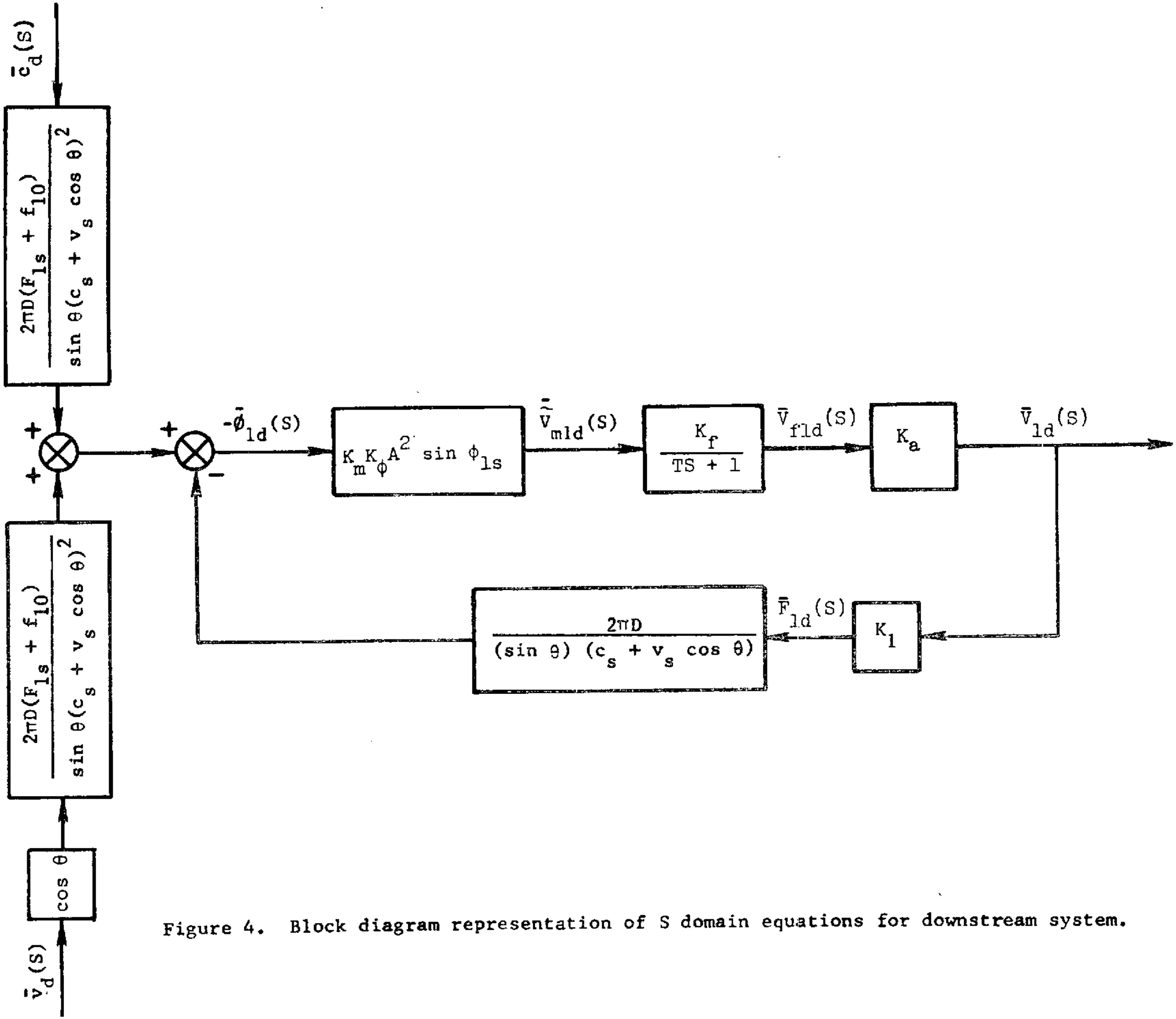

Figure 4. Block diagram representation of S domain equations for downstream system.

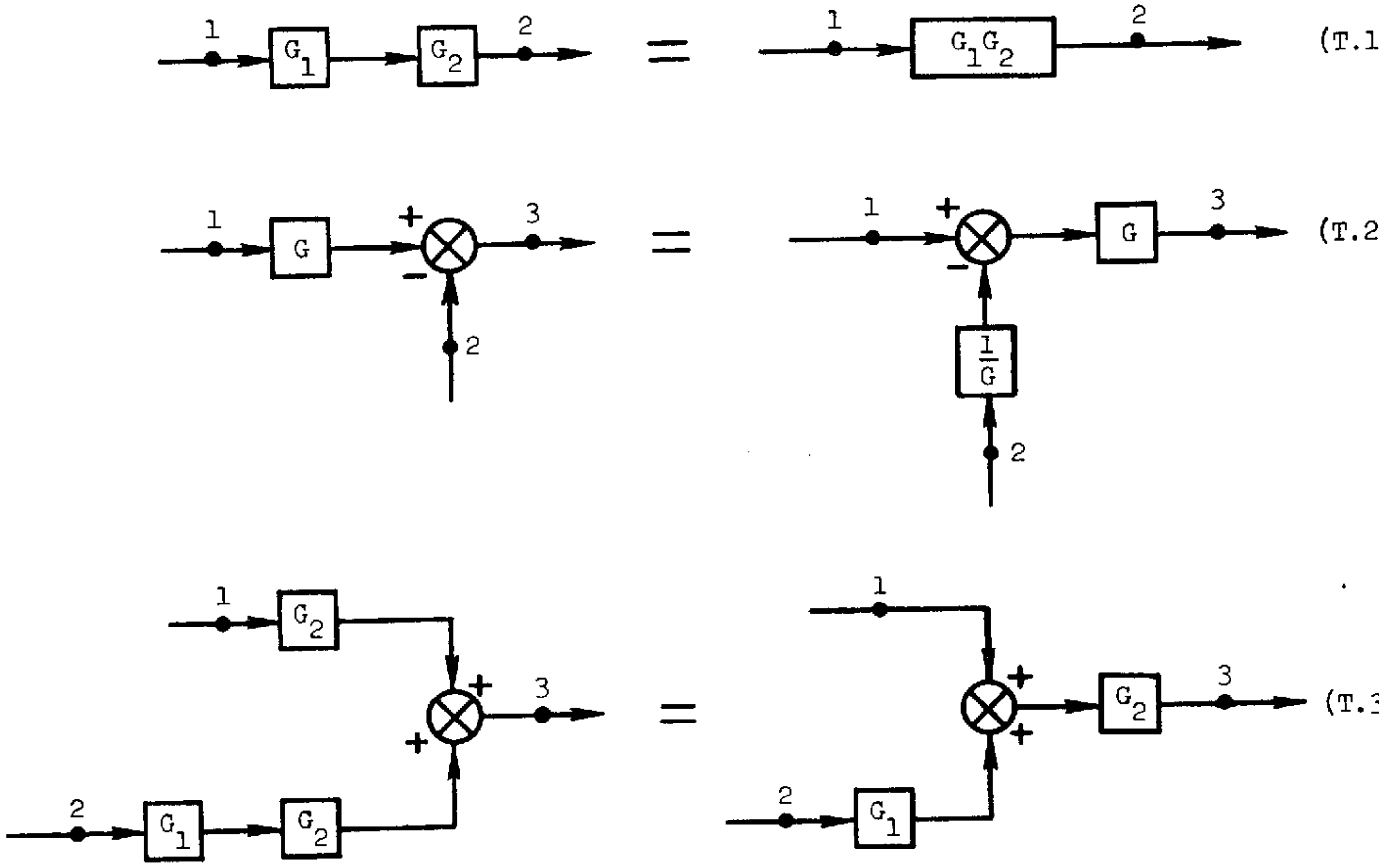

Figure 5. General block diagram transformations.

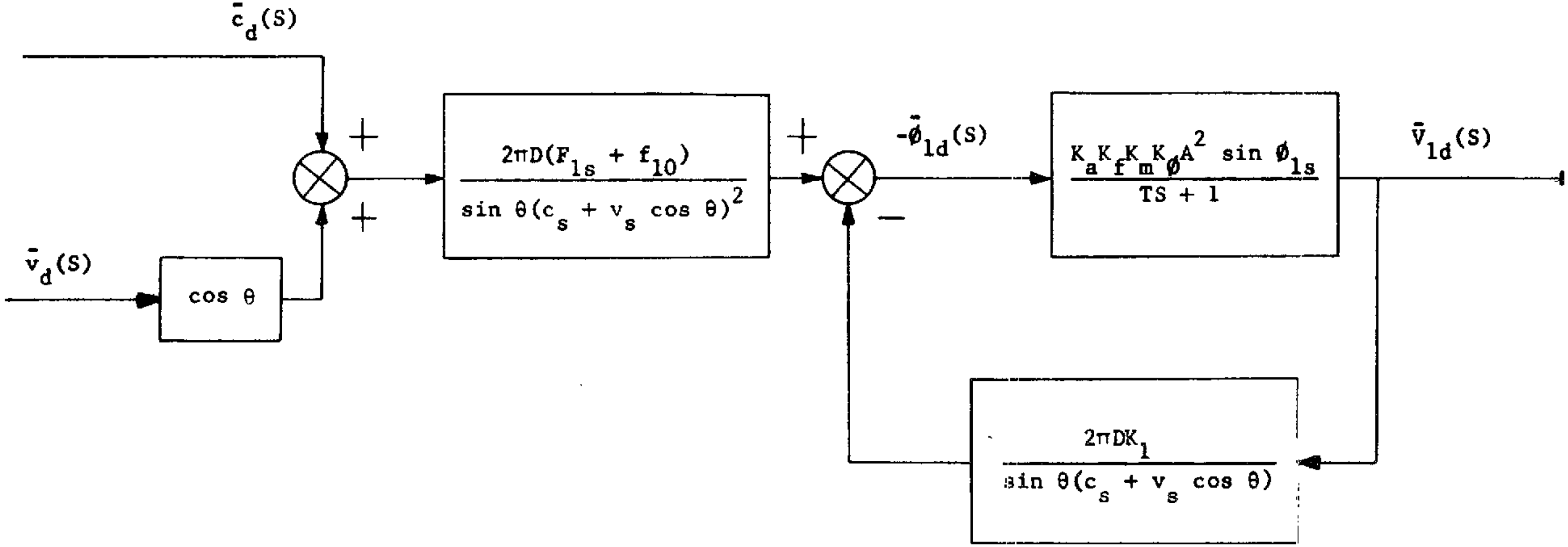

Figure 6. Block diagram derived from figure 4.

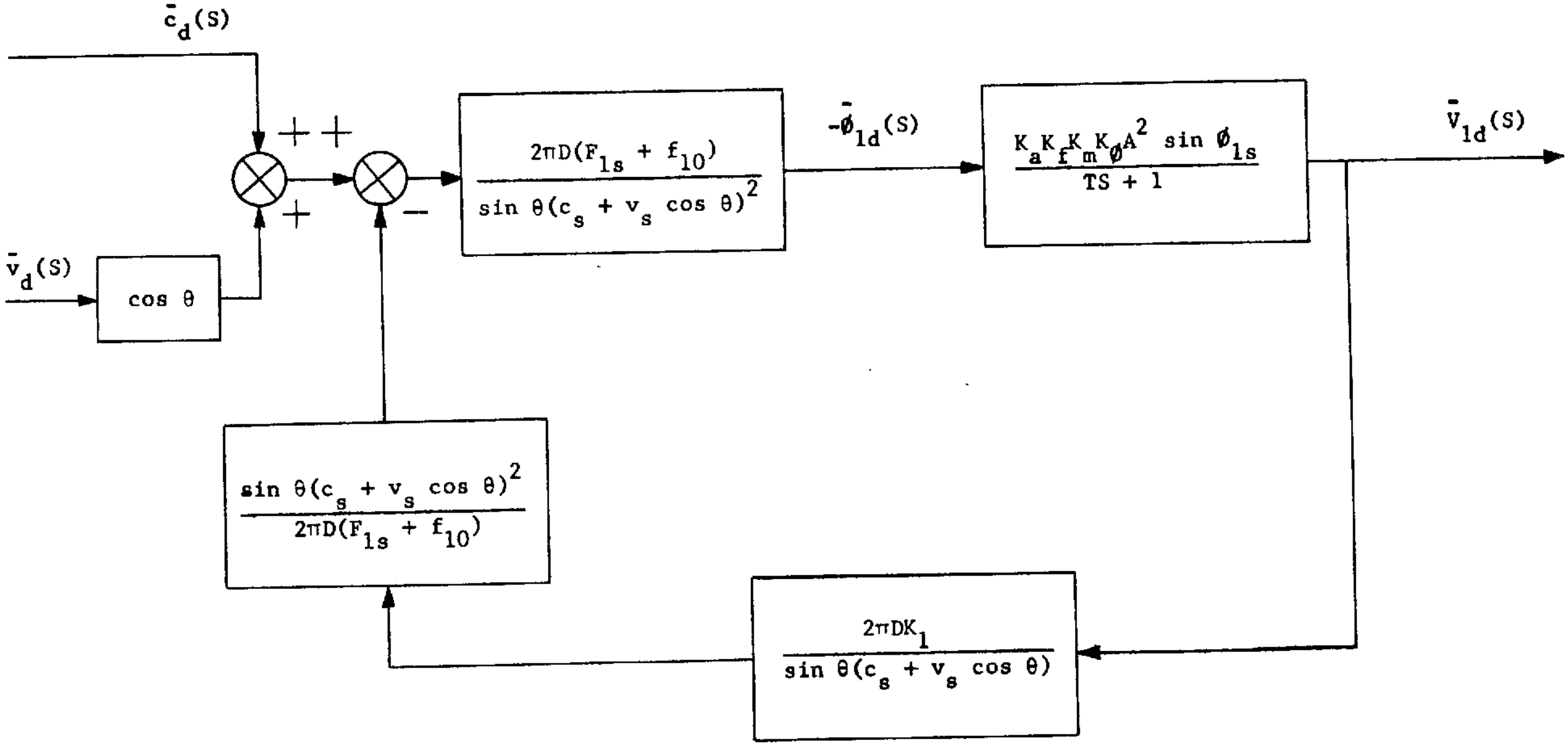

Figure 7. Block diagram derived from figure 6.

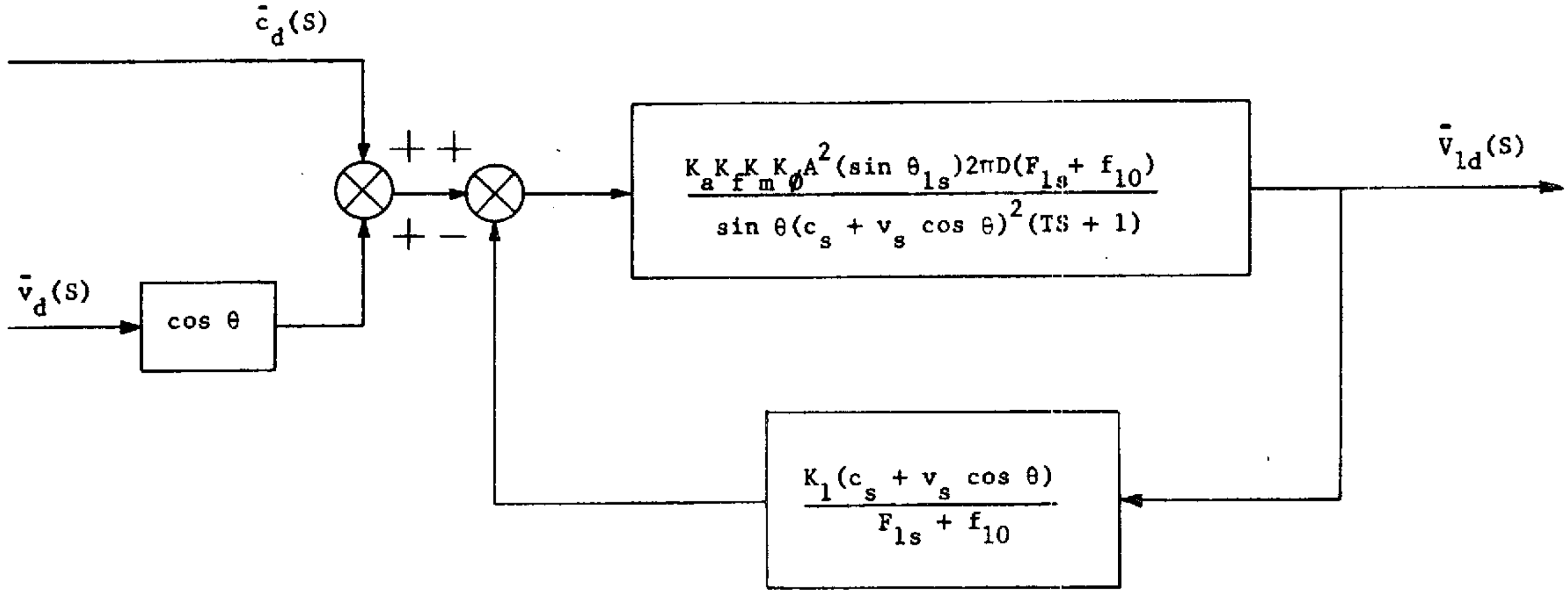

Figure 8. Downstream system block diagram derived from figure 7.

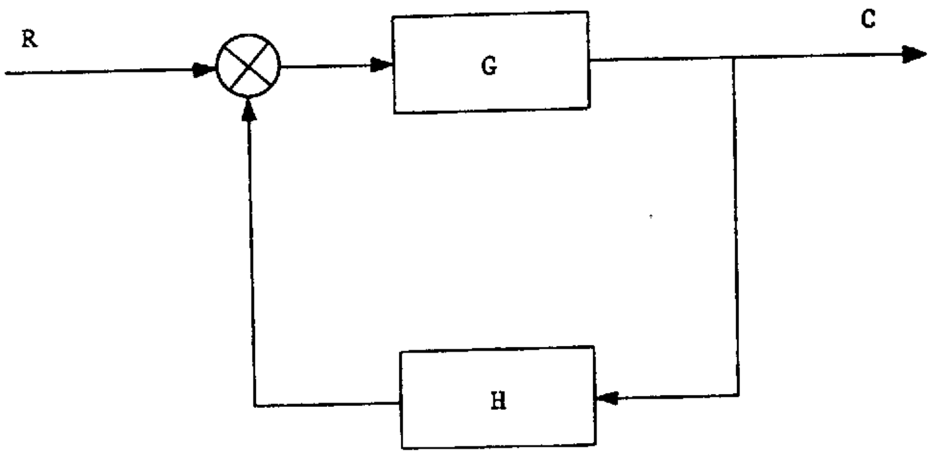

Figure 9. Block diagram for a negative feedback system.

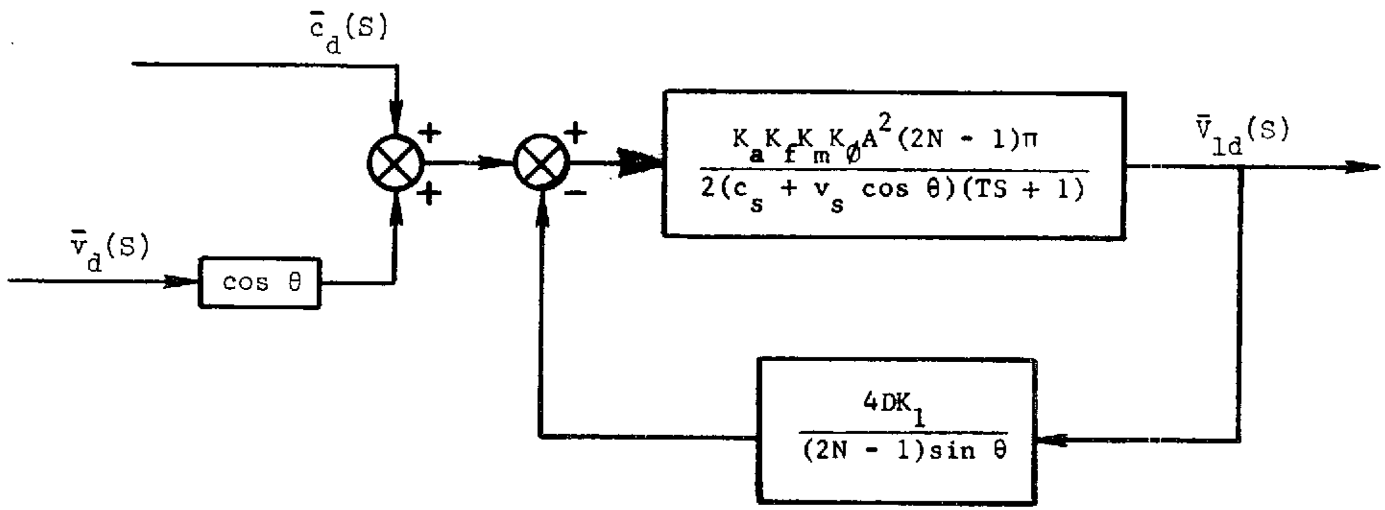

Figure 10. Downstream system block diagram derived from figure 8 by use of relationships $\sin \phi_{1s} \doteq 1$ and $F_{1s} + f_{10} \doteq (2N - 1)\sin\theta(c_s + v_s \cos\theta)/4D$.

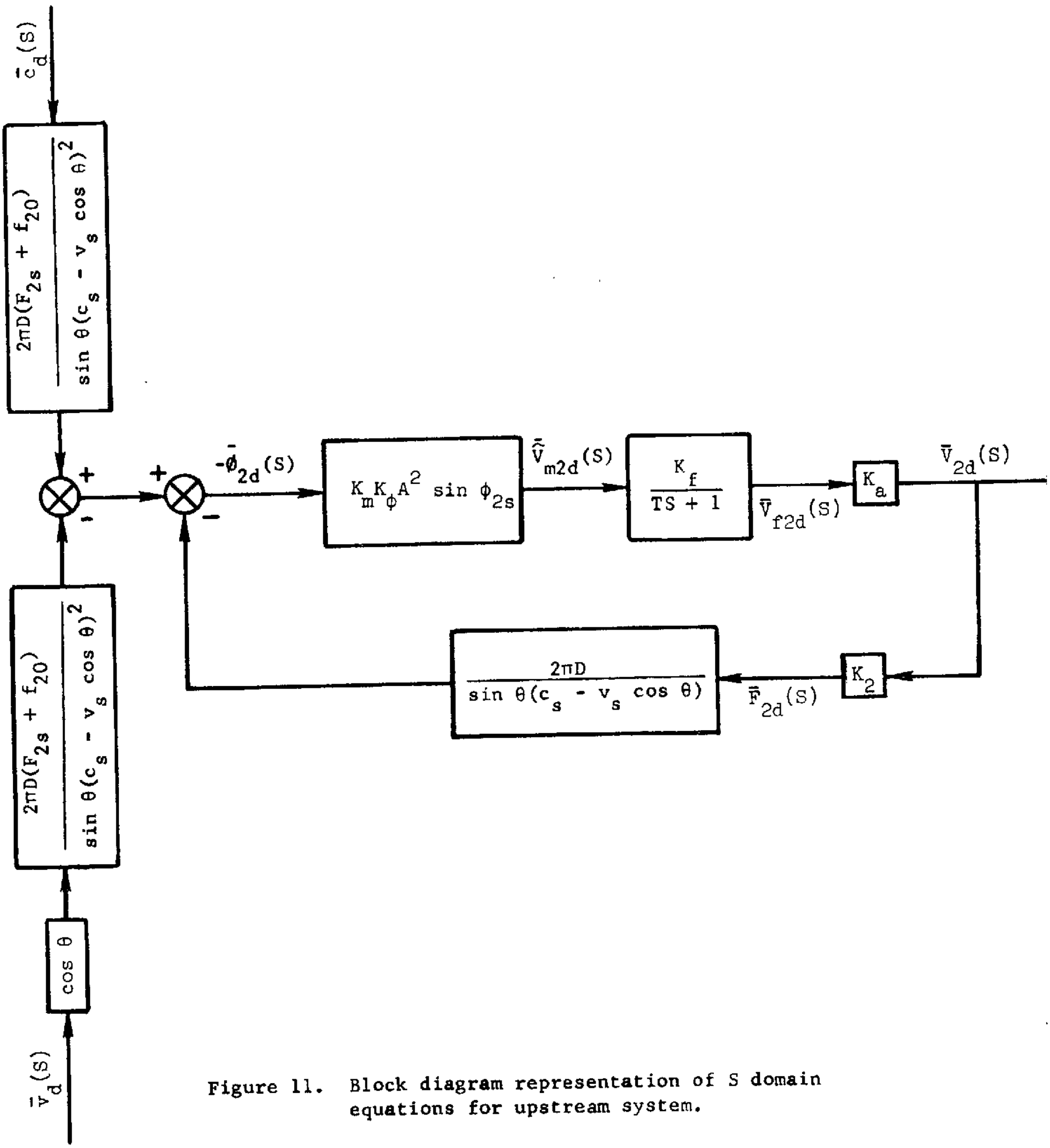

Figure 11. Block diagram representation of S domain equations for upstream system.

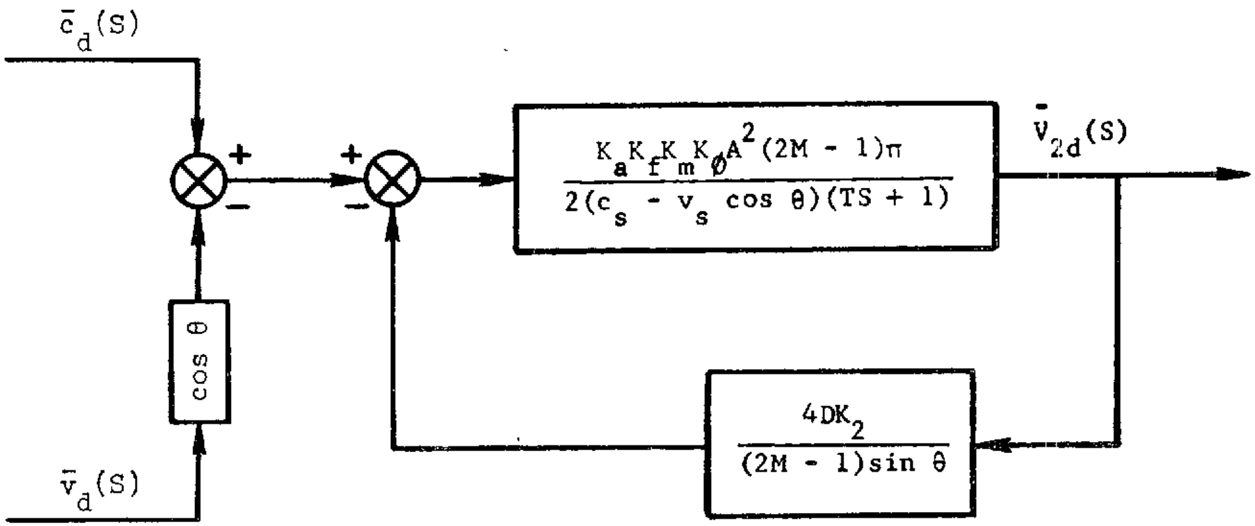

Figure 12. Upstream block diagram derived from figure 11.

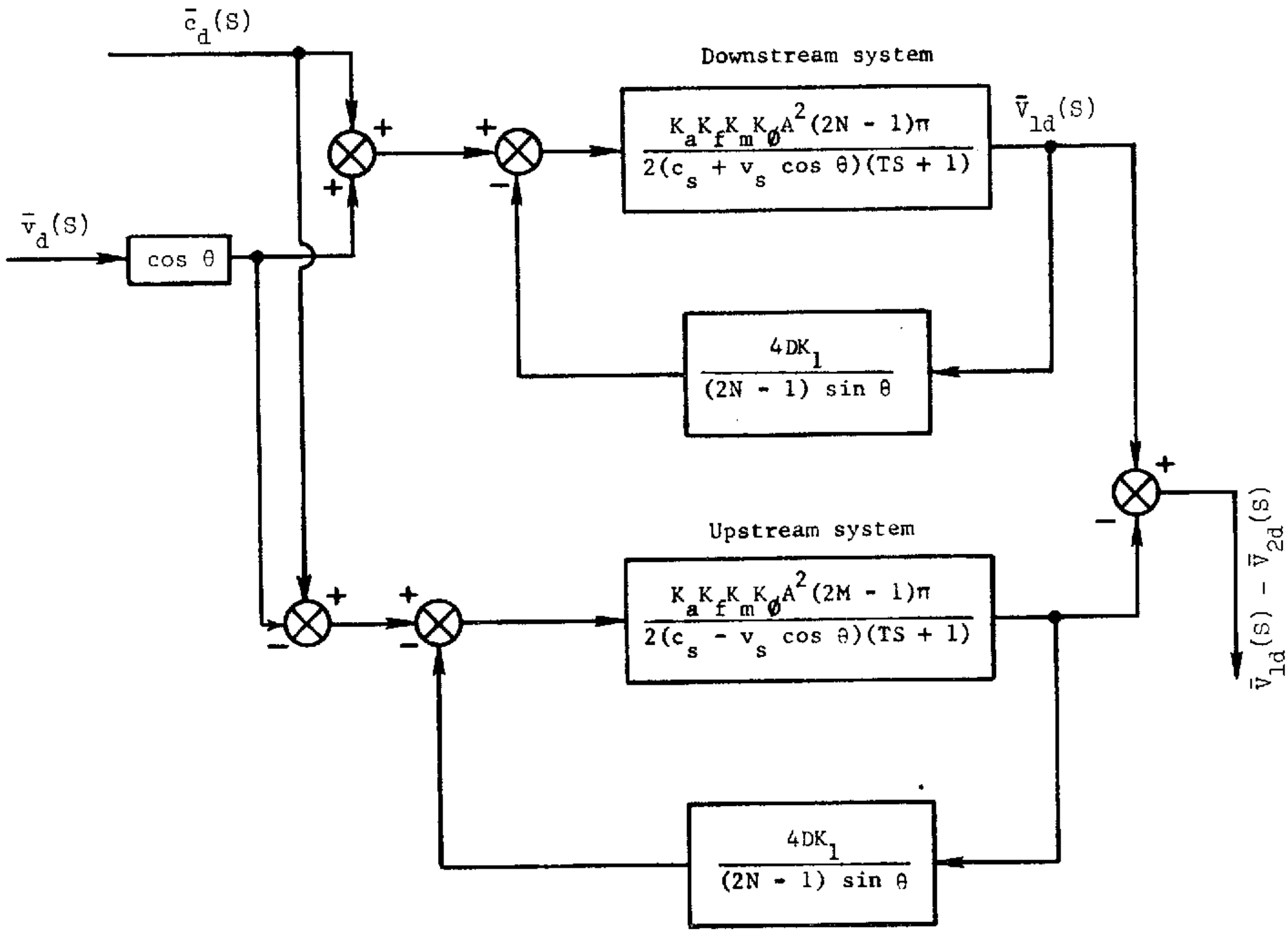

Figure 13. Block diagram for combined downstream and upstream systems.